

Mechanism and energetics of self-interstitial formation and diffusion in silicon

Ramakrishnan Vaidyanathan, Michael Y. L. Jung, and Edmund G. Seebauer*

Department of Chemical & Biomolecular Engineering, University of Illinois, Urbana, Illinois 61801, USA

(Received 20 March 2007; published 17 May 2007)

Recent work has suggested that prior determinations of diffusion mechanism and point defect thermodynamics in silicon have been affected by nonequilibrium effects stemming from uncontrolled adsorption-induced suppression of a pathway for defect creation at the surface. Through silicon self-diffusion measurements in ultrahigh vacuum in a short-time kinetic limit, the present work shows unambiguously that interstitials are the primary mediators of self-diffusion over the range 650–1000 °C, moving over distances of 5–9 nm before exchanging into the lattice. The Frank-Turnbull mechanism of interstitial formation does not play a significant role.

DOI: [10.1103/PhysRevB.75.195209](https://doi.org/10.1103/PhysRevB.75.195209)

PACS number(s): 61.72.Cc, 66.30.-h, 61.72.Ji

I. INTRODUCTION

Native point defects in silicon have been studied extensively for many years¹ to understand their diffusion and thermodynamics, which govern the growth of high-quality single crystals for most microelectronic devices^{2–4} as well as the doping processes required for their fabrication.^{5,6} Remarkably, considerable debate still surrounds the mechanism of Si self-diffusion,^{7–15} the question of whether interstitial atoms are the prime mediators (especially at temperatures below about 900 °C), the specific mechanism by which interstitials might operate, and the value of the interstitial formation energy. Computational approaches^{15–22} have not proven to be sufficiently reliable to resolve these questions, with calculated formation energies ranging from 2.2 to 4.5 eV. In this work, self-diffusion measurements exploiting a surface pathway for efficient defect formation show that interstitials are the primary mediators of self-diffusion over the range 650–1000 °C, moving over distances of 5–9 nm before exchanging into the lattice. The work also shows that interstitials mediate self-diffusion through a kick-out mechanism of exchange with the crystalline lattice, rather than a Frank-Turnbull mechanism of interstitial-vacancy creation.

Recent experiments in this laboratory have shown²³ that surface chemical bonding state affects the self-diffusion rate in silicon by influencing the concentration of point defects within the solid. Diffusion measurements have typically been made in the presence of surfaces whose dangling bonds are largely saturated with adsorbates of various kinds. However, maintaining an atomically clean surface opens a pathway for native point defect formation at the surface that is much more facile than corresponding pathways within the solid. The surface pathway fosters a much larger solid defect concentration on a several-hour laboratory time scale than in conventional approaches, with correspondingly larger self-diffusion rates. Data taken under clean conditions therefore yield substantially lower values for the defect formation energy.

II. EXPERIMENT

The present experiments employed atomically clean surfaces in conjunction with isotopic heterostructures.^{7,8} Layers

of silicon were grown epitaxially, by low-pressure chemical-vapor deposition, on Si substrates having a different ratio of the isotopes ²⁸Si and ³⁰Si. The natural isotope abundances in Si are 92.2% mass 28, 4.7% mass 29, and 3.1% mass 30. The concentration of ³⁰Si within the grown layer was 0.002%. Hence, a step concentration profile of ³⁰Si formed at the interface between the epitaxial layer and the substrate. These isotopic heterostructures were obtained as 4 in. *n*-doped wafers from Isonics Corporation. Arsenic served as the dopant and was present at a uniform level throughout the step-function structure at a concentration of $1 \times 10^{19} \text{ cm}^{-3}$. Specimen samples [within 1° of the (100) orientation] of approximate dimensions of $1.3 \times 0.7 \text{ cm}^2$ were cut from the wafers and degreased by successive 5 min rinsing cycles in electronic-grade trichloroethylene, acetone, and methanol. Native oxide was removed with 49% HF followed by rinsing in de-ionized water for 1 min. Temperature was monitored with a Chromel-Alumel thermocouple junction pressed into a small pit drilled into the specimen. Immediately thereafter, the specimens were mounted in the ultrahigh-vacuum chamber for resistive heating using Ta clips. The chamber was quickly pumped down to 10^{-9} torr to avoid significant native oxide formation. Auger electron spectroscopy verified that an atomically clean surface was maintained throughout the annealing process.

After annealing between 650 and 1000 °C, diffused ³⁰Si profile shapes were measured *ex situ* with secondary-ion-mass spectroscopy (SIMS) using a CAMECA IMS-5f instrument with a cesium ion beam. Other procedural details have been described elsewhere.²³

III. RESULTS

Most experiments employed a kinetic short-time limit.²⁴ This short-time limit circumvents a problem of data interpretation that has plagued most experimental work on Si self-diffusion. Typically, the spreading rate of isotopic concentration profiles has been measured to yield a composite diffusivity that incorporates parameters for native defect formation and migration. These parameters could not be separated, thereby leading to multiple possible interpretations of the data. In the short-time limit, however, fast-diffusing species (such as interstitial atoms) that occasionally exchange

TABLE I. Annealing conditions and fit parameters.

Sample No.	Annealing temperature (°C)	Annealing time (h)	Diffusion time regime	λ (nm)	K_{gen} (s ⁻¹)	D_{eff} (cm ² /s)
1	650	4	Short	8.2	1.7×10^{-7}	1.1×10^{-19}
2	650	4	Short	8.2	1.9×10^{-7}	1.3×10^{-19}
3	650	4	Short	8.1	2.2×10^{-7}	1.4×10^{-19}
4	700	1	Short	8.0	2.0×10^{-6}	1.3×10^{-18}
5	700	1	Short	8.1	2.0×10^{-6}	1.3×10^{-18}
6	700	1	Short	8.0	2.2×10^{-6}	1.3×10^{-18}
7	800	1	Short	7.1	8.4×10^{-5}	4.2×10^{-17}
8	800	1	Short	6.9	8.8×10^{-5}	4.2×10^{-17}
9	800	1	Short	7.0	8.5×10^{-5}	4.2×10^{-17}
10	900	1	Short	5.9	1.6×10^{-3}	5.6×10^{-16}
11	900	6	Intermediate	5.9	1.8×10^{-3}	6.3×10^{-16}
12	900	12	Intermediate	5.8	2.0×10^{-3}	6.7×10^{-16}
13	950	2	Intermediate	5.5	6.5×10^{-3}	2.0×10^{-15}
14	1000	6	Intermediate	5.0	3.0×10^{-2}	7.5×10^{-15}

with the lattice lead to exponential diffusion “tails” that evolve from initial delta-function²⁵ or step-function²⁴ profiles. A simple vacancy mechanism cannot yield such a signature in diffused profiles. Hence, although continuum diffusion profiles cannot be uniquely correlated to particular diffusion mechanisms,²⁶ certain mechanisms can be ruled out through suitable experimental design.

Note that some types of exponential tails can result from SIMS artifacts. For example, Ref. 27 shows exponential tails in isotope multilayer structures even before annealing. Well-defined steps were expected. The tails were ascribed to a SIMS artifact stemming from an ion-sputtered crater that was tilted with respect to the surface. That effect should not operate in the present work, however. If the present shapes were subject to this effect, then the exponential tails at all temperatures should have had the same slope. This pattern was evident in Ref. 27 but not in the present data. Furthermore, the ion-beam alignment, raster size, and detection area in the present work were chosen to avoid any significant sidewall contribution to the detected secondary ions. The sputtered crater depth was measured by stylus profilometry multiple times in both the length and width directions to ensure evenness of the crater bottom.

Profile fitting was performed using the series solution to the diffusion equations for mobile species as described in Ref. 24. This procedure yielded two parameters, namely, the mean path length λ between the generation and annihilation events of the fast-diffusing mobile species and the corresponding first-order rate constant K_{gen} for generation of this species. The effective diffusivity was computed from the relation $D_{eff} = K_{gen}\lambda^2$.²⁸ The initial step profile exhibited non-trivial spreading in the as-received wafers. A nonlinear least-squares fitting routine employed together with direct numerical solution of the diffusion equations²⁴ showed that the slight spreading present in the initial step profiles affected the calculated values of D_{eff} by no more than 10%.

In the short-time limit, the mean number of migration events (given by $K_{gen}t$) is less than about 1.²⁵ In this limit, it

was quite straightforward to obtain unique values for the parameters K_{gen} and λ . K_{gen} governs the “breakaway point” of the diffused profile from the initial step, whereas λ governs the slope of the exponential profile. As the diffusion time approaches infinity, the profile evolves asymptotically into a true complementary error-function shape.²⁵ In this long-time limit ($K_{gen}t \gg 1000$), the profile is completely described by the single parameter D_{eff} , which cannot be disaggregated into K_{gen} and λ from the profile alone. However, at intermediate times before the asymptotic limit is reached, K_{gen} and λ remain separable, although with progressively increasing uncertainty in the individual values. A few supplementary experiments were also done in this intermediate-time limit. Table I summarizes the experimental conditions in all regimes together with the parameters derived from the profile fitting.

Figure 1 shows typical ³⁰Si diffused profiles at 900 °C along with their corresponding analytical fits. Exponential tails are evident in the short-time data. At larger times, the profile shape evolves toward the true complementary error-

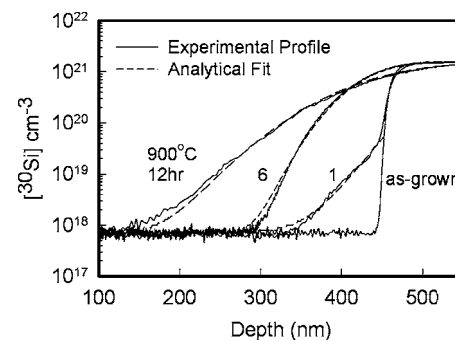


FIG. 1. Examples of SIMS profiles of ³⁰Si after diffusion at 900 °C for 1, 6, and 12 h. The 1 h profile is in the short-time limit, with an exponential tail. The other two profiles at 900 °C are in the intermediate-time limit.

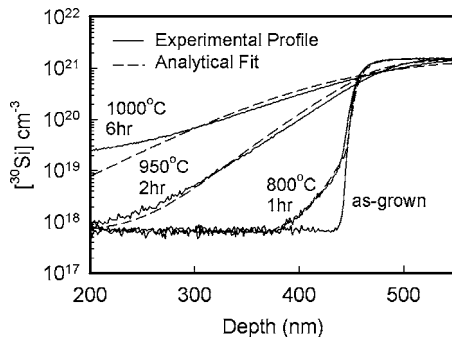


FIG. 2. Examples of SIMS profiles of ^{30}Si after diffusion at 800, 950, and 1000 °C. At 800 °C, the diffusion is in the short-time limit, with an exponential tail. The other two profiles at 950 and 1000 °C are in the intermediate-time limit.

function form. Figure 2 shows related data for several temperatures. Figure 3 focuses on shorter diffusion lengths at lower temperatures.

It was important to test for temporal effects in the effective diffusivity D_{eff} measured in the experiment. Temporal variations in D_{eff} would reflect time-dependent interstitial concentrations and affect the derived value of the formation energy. Indeed, Gossman *et al.* observed time-dependent changes in Si interstitial concentration within the solid during the spreading of doping superlattices under modest (10^{-7} torr) vacuum.²⁹ However, the adsorption state of the surface could not be directly monitored in those experiments, so the free dangling bond concentration at the surface could not be quantified.

The derived values of K_{gen} and λ obey an Arrhenius temperature dependence as shown in Fig. 4 and are given by

$$K_{gen} = 8 \times 10^{11} \exp[(-3.42 \pm 0.03) \text{ eV}/kT] \text{ s}^{-1} \quad (1)$$

and

$$\lambda = 1.3 \times 10^{-7} \exp[(0.15 \pm 0.01) \text{ eV}/kT] \text{ cm}, \quad (2)$$

where k represents Boltzmann's constant and T the temperature. The parameter λ ranges from roughly 5 to 9 nm in the

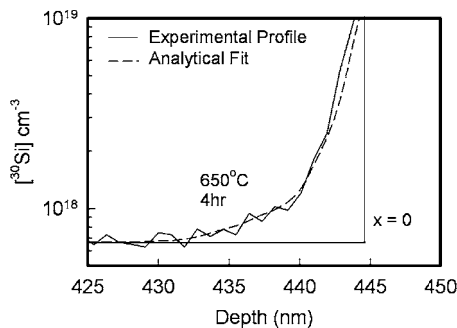


FIG. 3. SIMS profile of ^{30}Si after diffusion at 650 °C for 4 h. An exponential tail is observed in this short-time diffusion limit. A profile measured at 750 °C and 1 h lies almost exactly on top of the profile shown, with very similar shape. The $x=0$ location is also shown for the initial step profile.

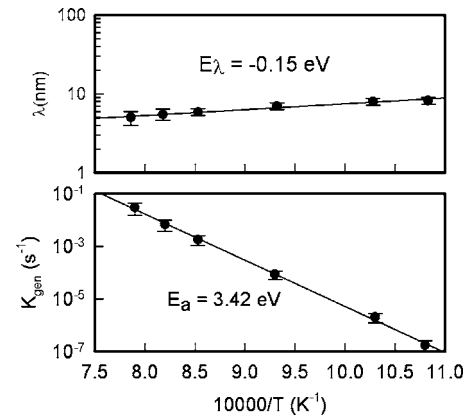


FIG. 4. Arrhenius plots for the mean path length λ and the generation rate parameter K_{gen} .

temperature range reported here. The effective diffusivity D_{eff} is hence given by

$$D_{eff} = 0.01 \exp[(-3.12 \pm 0.05) \text{ eV}/kT] \text{ cm}^2/\text{s}. \quad (3)$$

Figure 5 shows the effective diffusivities calculated for 900 °C as a function of time from 1 to 12 h. The plotted diffusivities include those estimated based on the equation $D_{eff} = K_{gen}\lambda^2$ at 900 °C and various annealing times between 1 and 12 h. The remaining values in Fig. 5 were calculated by converting the diffusivities obtained at other annealing temperatures to equivalent values at 900 °C using the activation energy of 3.12 eV in Eq. (3). D_{eff} remains constant within experimental error. These data indicate that the defect concentration does not change significantly over this time frame.

IV. DISCUSSION

A. Diffusion mechanism

The exponential shape at the lower temperatures and short anneal times gives clear evidence of a highly mobile intermediate species. A mechanism in which ^{30}Si atoms pair up with vacancies to diffuse in tandem could explain the data, in principle.^{24,28} However, such a mechanism seems unlikely in

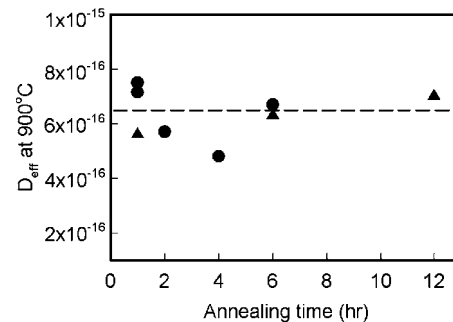


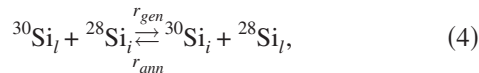
FIG. 5. D_{eff} at 900 °C as a function of annealing time. D_{eff} remains constant over this time scale. Triangles (▲) represent values taken at 900 °C. Circles (●) represent values of D_{eff} taken at other temperatures and converted to equivalent values at 900 °C using the activation energy of 3.12 eV.

the case of Si self-diffusion because there exists no obvious means for strong pairing. Such pairing has been postulated for diffusion of dopants in Si, where interaction between the vacancy and dopant atom arises from Coulombic attraction or possibly short-range elastic forces.¹² However, both of these interactions require the pairing atom to differ chemically from the host, so that differential charging and/or lattice distortion can take place. Although interstitials are commonly agreed to mediate diffusion in silicon above about 900 °C, there exists considerable debate over the diffusion mechanism below this temperature,^{8,9} with evidence being cited for both interstitials and vacancies. The present data show that when the surface pathway for defect formation functions efficiently, interstitials mediate diffusion in this lower-temperature range as well.

If interstitial atoms were created within the solid alone, the mere presence of exponential tails would be unable to distinguish between creation mechanisms involving vacancy-interstitial (or “Frank-Turnbull”) dissociation as opposed to kick-out, as has been shown by Marioton *et al.*³⁰ and Cowern.³¹ Distinguishing between the mechanisms would require variation of point defect concentrations in a controlled manner as outlined by Cowern *et al.*²⁸ However, the primary source of Si interstitials within the solid in the present case is the surface. Thus, most ³⁰Si interstitials responsible for profile evolution are created by direct exchange between ²⁸Si interstitials and ³⁰Si residing on lattice sites, akin to conventional kick-in/kick-out reactions. A Frank-Turnbull mechanism involving the formation of interstitials together with vacancies is not a major factor.

B. Energetics of lattice exchange

The exchange reaction between the interstitial and the lattice can be written as



where the subscripts *i* and *l* denote “interstitial” and “lattice.” The forward reaction rate r_{gen} refers to the generation of mobile interstitials of the minority atom (³⁰Si), and the backward reaction rate r_{ann} refers to the annihilation of this interstitial species. We assume that the forward generation reaction obeys the expression

$$r_{gen} = k_{gen} [{}^{28}\text{Si}_i] [{}^{30}\text{Si}_l] = K_{gen} [{}^{30}\text{Si}_l], \quad (5)$$

where $K_{gen} = k_{gen} [{}^{28}\text{Si}_i]$. Similarly, the reverse annihilation reaction obeys

$$r_{ann} = k_{ann} [{}^{28}\text{Si}_i] [{}^{30}\text{Si}_l] = K_{ann} [{}^{30}\text{Si}_l], \quad (6)$$

where $K_{ann} = k_{ann} [{}^{28}\text{Si}_i]$. With the assumption of no significant kinetic isotope effects, we set $k_{ann} = k_{gen}$.

The rate parameters in Eqs. (5) and (6) were obtained from the parameters in Eqs. (1) and (2). The mean hop length $\lambda = (D_{hop}/K_{ann})^{1/2}$, where D_{hop} represents the diffusivity for site-to-site hopping of the Si interstitial (of either isotope, again assuming no kinetic isotope effect). The parameter k_{gen} can be calculated from the experimental data for λ together

with an estimate for D_{hop} and the ²⁸Si lattice density [²⁸Si]_l = 5 × 10²² cm⁻³. For D_{hop} , the activation energy has been estimated using maximum likelihood methods from a wide variety of literature reports to be 0.72 ± 0.03 eV,³² while the pre-exponential factor was assumed to be 1 × 10⁻³ cm²/s. This procedure yields

$$k_{gen} = 1.2 \times 10^{-12} \exp(-1.02 \text{ eV}/kT) \text{ cm}^3/\text{s}. \quad (7)$$

Equation (7) in combination with Eq. (1) for K_{gen} yields

$$[{}^{28}\text{Si}_i] = 6.8 \times 10^{23} \text{ cm}^{-3} \exp(-2.4 \text{ eV}/kT). \quad (8)$$

This expression yields an enthalpy of interstitial formation of 2.4 eV and a normalized entropy $\Delta S/k$ of 2.6. The value of $\Delta S/k$ is modest and is not unusual for a formation entropy, but the computed enthalpy is much lower than most reported values.

Most quantum calculations^{15,18–20,33,34} report a formation energy for the neutral interstitial in the range of 3.3–4.5 eV, although there are a few exceptions with much lower values. (The formation energy of the silicon interstitial depends on its charge state, though for the modestly *n*-type silicon used in our experiments, the interstitial is probably in the neutral state.³⁵) A wide variety of diffusion mechanisms have been propounded. The studies differ in the details of the computational method, and indeed there is considerable debate over the best method to use because the combination of strong and weak bonds in many interstitial configurations poses significant challenges for electronic structure calculations.^{20,22,36}

Two studies give formation energies close to the 2.4 eV observed in this laboratory. Goedecker *et al.*²¹ reported a quadruply coordinated configuration at 2.4 eV, but indicate that this structure does not participate in diffusion. Clark and Ackland¹⁶ reported a low-symmetry caged structure (akin to a distorted split-⟨110⟩ interstitial) having a formation energy of 2.2 eV. Our results accord well with this value. The calculations indicated that the diffusing interstitial can move from cage to cage without lattice exchange, but can also undergo lattice exchange into a higher-symmetry split-⟨110⟩ (“dumbbell”) configuration. The presence of exponential tails in the experiments helps us to distinguish among these site-to-site hopping mechanisms; the long path length of 5–9 nm indicates that lattice exchange is relatively infrequent compared to diffusion without lattice exchange.

Subsequent calculations by Leung *et al.*²⁰ and Needs¹⁹ did not confirm the stability of the caged structure, but instead reported the higher-symmetry split-⟨110⟩ and hexagonal configurations as having the lowest formation energies of 3.3 eV (in the local-density approximation) and 3.8 eV (in the generalized gradient approximation). The results also pointed to two diffusion mechanisms: one involving repeated lattice exchange and another involving diffusion between hexagonal sites without lattice exchange. Although the present experimental results do not conflict with the predicted diffusion mechanisms, the formation energies indicated by the calculations are much higher than those observed here. Marques *et al.*²² reported the tetrahedral structure as the most stable with a formation energy of 3.45 eV, but all their diffusion mechanisms involve lattice exchange.

The present estimate for the formation energy depends on the accuracy of the parameters employed for site-to-site diffusion. Reference 32 gives a lengthy discussion of this issue, and the parameters employed here are the best available, but independent checks on the parameters derived here would be useful. One such check is the 1.02 eV activation energy calculated for exchange of the Si interstitial with the lattice. This reaction resembles the kick-out of dopants, for which data exist. For example, for a small, covalently bonded element such as boron, the activation energy for kick-out based on experiments and quantum calculations is 1.05 eV,³² very similar to the number reported here.

V. CONCLUSION

Self-diffusion experiments in silicon with isotopic profile decay in the presence of an atomically clean surface, and in the short-time kinetic limit show that the mechanism is me-

diated primarily by interstitial atoms over the broad temperature range 650–1000 °C and involves migration over a long path length of 5–9 nm with occasional lattice exchange. A Frank-Turnbull mechanism involving simultaneous creation of interstitials and vacancies in the bulk does not play a significant role. The interstitial formation energy is estimated to be 3.12 eV, which is significantly lower than the values reported earlier in literature.

ACKNOWLEDGMENTS

This work was partially supported by NSF (CTS 02-03237) and the ACS PRF (43651-AC5). SIMS was performed at the UIUC Center for Microanalysis of Materials, which is partially supported by the U.S. Department of Energy under Grant No. DEFG02-96-ER45439. We thank Jinju Lee and Tim Spila for their help with SIMS profiling and Steve Burdin at Isonics Corp. for overseeing the creation of isotopically labeled specimens.

*Corresponding author. Email address: eesebaue@uiuc.edu

¹P. Pichler, *Intrinsic Point Defects, Impurities, and Their Diffusion in Silicon* (Springer, New York, 2004).

²W. Wijaranakula, *J. Electrochem. Soc.* **139**, 604 (1992).

³R. Habu, T. Iwasaki, H. Harada, and A. Tomiura, *Jpn. J. Appl. Phys., Part 1* **33**, 1234 (1994).

⁴S. Takeda, M. Kohyama, and K. Ibe, *Philos. Mag. A* **70**, 287 (1994).

⁵P. M. Fahey, P. B. Griffin, and J. D. Plummer, *Rev. Mod. Phys.* **61**, 289 (1989).

⁶P. Shewmon, *Diffusion in Solids* (Minerals, Metals, & Materials Soc., Warrendale, PA, 1989).

⁷H. Bracht, E. E. Haller, and R. Clark-Phelps, *Phys. Rev. Lett.* **81**, 393 (1998).

⁸A. Ural, P. B. Griffin, and J. D. Plummer, *Phys. Rev. Lett.* **83**, 3454 (1999).

⁹H. Bracht, N. A. Stolwijk, and H. Mehrer, *Phys. Rev. B* **52**, 16542 (1995).

¹⁰B. J. Masters and J. M. Fairfield, *Appl. Phys. Lett.* **8**, 280 (1966).

¹¹W. Frank, U. Goesele, H. Mehrer, and A. Seeger, in *Diffusion in Crystalline Solids*, edited by G. E. Murch and A. S. Nowick (Academic, New York, 1984).

¹²R. B. Fair, in *Silicon Integrated Circuits*, edited by D. Kahng (Academic, New York, 1981), Pt. B.

¹³B. L. Sharma, *Defect Diffus. Forum* **70-71**, 1 (1990).

¹⁴K. C. Pandey, *Phys. Rev. Lett.* **57**, 2287 (1986).

¹⁵P. E. Blöchl, E. Smargiassi, R. Car, D. B. Laks, W. Andreoni, and S. T. Pantelides, *Phys. Rev. Lett.* **70**, 2435 (1993).

¹⁶S. J. Clark and G. J. Ackland, *Phys. Rev. B* **56**, 47 (1997).

¹⁷J. A. Van Vechten, *Phys. Rev. B* **33**, 2674 (1985).

¹⁸T. Sinno, K. Jiang, and A. Brown, *Appl. Phys. Lett.* **68**, 3028 (1996).

¹⁹R. J. Needs, *J. Phys.: Condens. Matter* **11**, 10437 (1999).

²⁰W.-K. Leung, R. J. Needs, G. Rajagopal, S. Itoh, and S. Ihara,

Phys. Rev. Lett. **83**, 2351 (1999).

²¹S. Goedecker, T. Deutsch, and L. Billard, *Phys. Rev. Lett.* **88**, 235501 (2002).

²²L. A. Marques, L. Pelaz, P. Castrillo, and J. Barbolla, *Phys. Rev. B* **71**, 085204 (2005).

²³E. G. Seebauer, K. Dev, M. Y. L. Jung, R. Vaidyanathan, C. T. M. Kwok, J. W. Ager, E. E. Haller, and R. D. Braatz, *Phys. Rev. Lett.* **97**, 055503 (2006).

²⁴R. Vaidyanathan, M. Y. L. Jung, R. D. Braatz, and E. G. Seebauer, *AICHE J.* **52**, 366 (2006).

²⁵N. E. B. Cowern, K. T. F. Janssen, G. F. A van de Walle, and D. J. Gravesteijn, *Phys. Rev. Lett.* **65**, 2434 (1990).

²⁶A. Ural, P. B. Griffin, and J. D. Plummer, *Phys. Rev. B* **65**, 134303 (2002).

²⁷H. Bracht, H. H. Silvestri, I. D. Sharp, S. P. Nicols, J. W. Beeman, J. L. Hansen, A. Nylandsted, and E. E. Haller, *Inst. Phys. Conf. Ser.* **171**, C3.8 (2003).

²⁸N. E. B. Cowern, G. F. A. van de Walle, D. J. Gravesteijn, and C. J. Vriezema, *Phys. Rev. Lett.* **67**, 212 (1991).

²⁹H. J. Gossman, C. S. Rafferty, F. C. Unterwald, C. Boone, T. K. Mogi, M. O. Thompson, and H. S. Luftman, *Appl. Phys. Lett.* **67**, 1558 (1995).

³⁰B. P. R. Marioton, U. Goesele, and T. Y. Tan, *Chemtronics* **1**, 156 (1986).

³¹N. E. B. Cowern, *J. Appl. Phys.* **64**, 4484 (1988).

³²M. Y. L. Jung, R. Gunawan, R. D. Braatz, and E. G. Seebauer, *AICHE J.* **50**, 3248 (2004).

³³M. Tang, L. Colombo, J. Zhu, and T. Diaz de la Rubia, *Phys. Rev. B* **55**, 14279 (1997).

³⁴W. C. Lee, S. G. Lee, and K. J. Chang, *J. Phys.: Condens. Matter* **10**, 995 (1998).

³⁵M. Y. L. Jung, C. T. M. Kwok, R. D. Braatz, and E. G. Seebauer, *J. Appl. Phys.* **97**, 063520 (2005), and references therein.

³⁶P. A. Schultz, *Phys. Rev. Lett.* **96**, 246401 (2006).